THE EXPANSION OF THE X-RAY REMNANT OF TYCHO'S SUPERNOVA (SN1572)

John P. Hughes
Department of Physics and Astronomy, Rutgers University, 136 Frelinghuysen Road, Piscataway, NJ
08854-8019 jph@physics.rutgers.edu

ABSTRACT

Two *ROSAT* high resolution images separated by nearly five years have been used to determine the expansion of the X-ray remnant of Tycho's supernova (SN1572). The current expansion rate averaged over the entire remnant is $0.124 \pm 0.011 \% \, \mathrm{yr}^{-1}$, which, when combined with the known age of the remnant, determines the mean expansion parameter m, defined as $R \propto t^m$, to be 0.54 ± 0.05. There are significant radial and azimuthal variations of the X-ray expansion rate. The radial expansion in particular shows highly significant evidence for the more rapid expansion of the forward blast wave as compared to the reverse-shocked ejecta, an effect that has not been seen previously. The expansion parameter varies from $m = 0.71 \pm 0.06$ at the outermost edge of Tycho's supernova remnant (SNR) to a value of $m = 0.34 \pm 0.10$ on the inside edge of the bright rim of emission. These values are consistent with the rates expected for a remnant with constant density ejecta evolving into a uniform interstellar medium during the ejecta-dominated phase of evolution. Based on the size, age, and X-ray expansion rates, I obtain values for the explosion energy and ambient density of $E \approx 4 - 5 \times 10^{50}$ ergs and $n_0 \approx 0.35 - 0.45 \, \mathrm{cm}^{-3}$. As is also the case for Cas A and Kepler's SNR, the X-ray expansion rate of Tycho's SNR appears to be significantly higher than the radio expansion rate. In the case of Tycho's SNR, however, the difference between radio and X-ray expansion rates is clearly associated with the motion of the forward shock.

Subject headings: ISM: individual (Tycho's Supernova) – shock waves – supernova remnants – X-rays: ISM

1. INTRODUCTION

Measurement of the current rate of expansion provides essential information on the dynamical state of supernova remnants (SNRs). This is particularly true for the so-called historical remnants, those for which the date of the supernova (SN) explosion is known, since a comparison of the average expansion rate with the current expansion rate yields a measure of the deceleration. Unfortunately, the rate of expansion, although rapid compared to most astrophysical objects in the cosmos, is still rather long on human timescales, necessitating measurements over the course of years, if not decades, in order to attain accurate results. *ROSAT* was the first X-ray observatory that had sufficient angular resolution ($\sim 4''$ half-power radius for the High Resolution Imager) and operated for a long enough time that significant measurements of the expansion rate of young SNRs are possible.

The time-averaged expansion rate of Tycho's SNR based on the outermost extent of the remnant ($\sim 8'$ in diameter) in either the radio or X-ray band and its well-known age is $\sim 0''.56 \, \mathrm{yr}^{-1}$. The observed proper motion of the optical filaments, which are believed to trace the location of the blast wave, indicate much lower current expansion rates ranging from $0''.18 \, \mathrm{yr}^{-1}$ to $0''.28 \, \mathrm{yr}^{-1}$ (Kamper & van den Bergh 1978). Evidently these filaments are locations where significant deceleration of the SN blast wave has occurred. From the width of the broad Hα emission Smith et al. (1991) derive shock velocities in the range 1500–2800 km s^{-1} that, when combined with the proper motion measurements, imply a distance of 1.5–3.1 kpc. This range is in good agreement with other distance estimates to the remnant (Green 1984; however, see Schwarz et al. 1995) and in the following I adopt a value of 2.3 kpc for the dis-

tance. Because the optical filaments cover only a limited portion of Tycho's SNR, the optical data are unable to provide a comprehensive picture of the expansion of the remnant.

The radio remnant of Tycho's SN has also been observed to be expanding at the current epoch (Strom, Goss, & Shaver 1982; Tan & Gull 1985; Reynoso et al. 1997, hereafter R97). Although in each successive analysis the radio data have improved, the basic result of these studies have remained in general agreement. The current radio expansion rate, averaged over the outer rim, is $0.113 \% \, \mathrm{yr}^{-1}$ or, expressed equivalently, the expansion parameter, defined as $R \propto t^m$, is $m = 0.471 \pm 0.028$. This result is between the free expansion rate, $m \sim 1$, and the expansion rate expected for a remnant in the Sedov phase of evolution, $m = 0.4$. There is significant azimuthal variation of the radio expansion rate, while interior features appear to show the same expansion rate as the rim (R97).

Vancura, Gorenstein, & Hughes (1995), using data from two satellite observatories, quoted a current X-ray expansion rate for the SNR based on a 11.5 yr time baseline that was consistent with these other values. Here I present more accurate results on the X-ray expansion of Tycho's SNR using high resolution images accumulated by the *ROSAT* satellite in two epochs separated by 4.55 yr. A preliminary report on this work, using a different analysis approach, was given by Hughes (1997).

2. OBSERVATIONS

The reduction of the X-ray data closely follows that done in an earlier study of Kepler's SNR (Hughes 1999, hereafter H99); interested readers are referred there for more

details. A log of the high resolution *Einstein*[1] and *ROSAT* imaging observations of Tycho's SNR is given in Table 1. The columns list the observatory, start date, the Modified Julian Day (MJD) corresponding to the average date of the observation, and the effective duration (live-time corrected). Figure 1 shows the image from observation R2.

TABLE 1
OBSERVATIONS OF TYCHO'S SNR

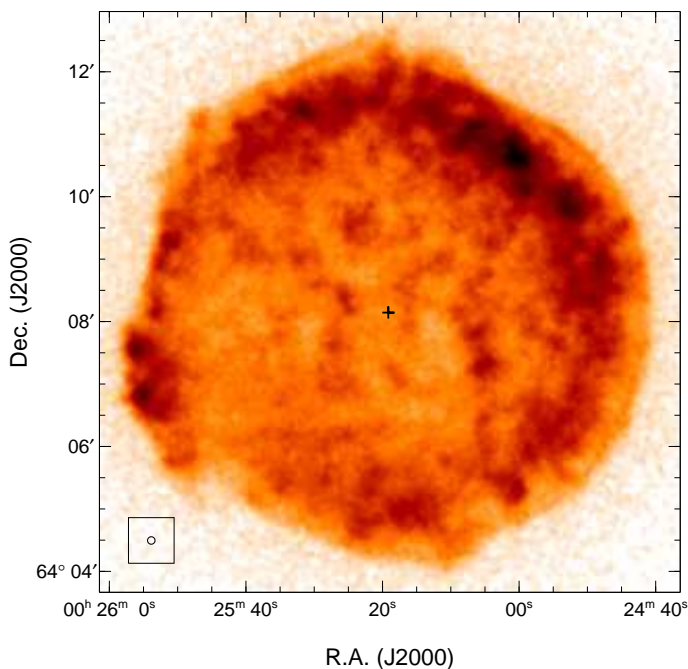| Observatory	Start Date	Ave. MJD	Duration (s)
Einstein	1979 Feb 8	43,913.3	50409.2
ROSAT (R1)	1990 Jul 28	48,100.7	22163.7
ROSAT (R2)	1995 Feb 5	49,763.7	104332.1

FIG. 1.— *ROSAT* HRI image of Tycho's SNR. The data were smoothed by a Gaussian function with $\sigma = 2''$ and are displayed with a square-root intensity scaling. The plus sign marks the geometric center of the remnant. The effective resolution of the map, including both the instrumental point-spread function and the average width of the smoothing kernel, is shown at the lower left.

The *ROSAT* high resolution imager (RHRI) data were processed in some detail. The data were filtered in pulse height to reduce background. Pulse height channels 1 to 11 were used for the first epoch *ROSAT* observation (R1) and channels 1 to 12 were used for the second epoch observation (R2). This reduced the background level by 5%-7% while the source rates were nearly unaffected ($\sim$1% change). Aspect drift throughout an observation was corrected by aligning separate images made from the data corresponding to each orbit. The images from all the sub-intervals (typically 1500 s long) were registered to the nearest $0''.5$ pixel, shifted, and added. For R1 the initial registration of the individual maps from the standard analysis was fairly good: all of the individual maps were already

aligned relative to each other to within $\sim 2''$ or better. In the case of R2 there was clear evidence for a drift in aspect throughout the observation. The mean registration error was $\sim 3''$, although some of the individual images were misregistered by up to $10''$. For both epochs, the shift-and-add alignment technique produced images with a noticeably improved point response function.

The grain scattering halo from Tycho's SNR (Mauche & Gorenstein 1986; Predehl & Schmitt 1995) extends over the entire field of view of the HRI, which makes background estimation difficult. The background level was estimated by fitting a spatial power-law component (for the scattering halo) plus a constant background level to the surface brightness profile over the $5'$ to $15'$ radial range. The fitted power-law components were consistent between the two RHRI pointings (index of -2.3), although the background levels differed by some 15%, 4.2×10^{-3} cts s^{-1} arcmin^{-2} for R1 and 3.7×10^{-3} cts s^{-1} arcmin^{-2} for R2. This difference is within the variation observed from field to field for the RHRI (David et al. 1998).

Exposure maps were generated for the RHRI observations as before (see H99). Over the portion of the field containing the image of the remnant the ratio of exposure between the first and second epochs varied between 0.963 and 1.045. These corrections are small in comparison to the flux differences I measure and are uncorrelated with image structure in the remnant. Nevertheless, these maps are included in the model fits described below.

The exposure- and deadtime-corrected, background-subtracted RHRI count rates of Tycho's SNR within a radius of $8'$ are $9.092 \pm 0.020\,\text{s}^{-1}$ and $9.209 \pm 0.009\,\text{s}^{-1}$ from the first and second epoch images, respectively. This difference in count rates ($\sim$1%) is consistent with the range of RHRI rates seen in calibration observations of the SNR N132D (see H99).

Finally I comment on possible changes in the plate scale using observations of the Andromeda galaxy, which was observed by the RHRI in July 1990, 1994, and 1995, and January 1996. I extracted these data and used the positions of 10 isolated, moderately bright X-ray point sources to constrain the relative rotation angle and plate scale change between pairs of observations. I find no evidence for a change in the RHRI plate scale and set a limit of $\sim$0.008% yr^{-1} on any changes for timescales of 4 yrs or more.

3. EXPANSION RESULTS

The expansion rate was determined using fitting software that takes one image ("model") and compares it to another ("data") as described in H99. The model image was scaled in intensity, shifted in position, and expanded (or contracted) in spatial scale to match the data using, as the figure-of-merit function, the maximum likelihood statistic for Poisson-distributed data. The fitted spatial scale factor yields the global mean expansion rate, which is assumed to be uniform across the entire remnant.

Over the 4.55 yrs between observations R1 and R2, Tycho's SNR expanded annually by an amount 0.124 ± 0.011 % yr^{-1}. The error bar is statistical at $1\,\sigma$ and includes uncertainty from Poisson noise in both observations

---

[1]The *Einstein* observation is included here for completeness and in fact results for only the two *ROSAT* data sets are presented below. Preliminary studies found that the *Einstein*/*ROSAT* expansion results were inconsistent with the *ROSAT*/*ROSAT* ones, yielding expansion values a factor of 1.6–1.9 times higher. The *Einstein* and *ROSAT* comparison is subject to more uncertainty due to differences in the instrumental point-spread functions and spectral bandpasses. The latter effect, combined with spatial variations in the X-ray spectrum of Tycho's SNR (Vancura et al. 1995), is the likely cause of the discrepancy.

as well as plate scale changes assuming the limit given above. This result is highly significant both in terms of the final error bar and the reduction in the value of the likelihood statistic for fits with and without any expansion.

In order to determine the expansion rate as a function of radius and azimuthal angle, one needs to know the position of the expansion center. The current X-ray data do not allow for the determination of this quantity (see H99), so I have opted to just define the geometric center of the remnant at $0^h25^m19^s$ $64°08'10''$ (J2000) as the nominal center of expansion. I then investigated how the results depended on this choice by varying the center position by $40''$ in each of the four cardinal directions. I found that the different choices of center could be nearly perfectly compensated for by appropriate choices of the relative alignment of the two images. (Since there were no serendipitous point sources in the field, it was not possible to do an independent registration of the images.) This result is not surprising since non-optimal image alignment or choice of expansion center will each introduce a sinusoidal term in the expansion rate as a function of azimuth. In effect what I have done is to remove any such sinusoidal term from the results, regardless of origin. My approach is different from that of R97 who used a fixed expansion center (defined by the center of the nearly circular western limb) to measure the radio expansion of Tycho's SNR. And indeed their fractional expansion results do contain a significant sinusoidal term. Because of these complications a detailed comparison between the X-ray and published radio azimuthal variation is not particularly enlightening and will not be pursued in this work. However, since a sinusoid averages to zero over a full cycle, this difference does not affect the comparison of the radio and X-ray global mean expansion rates. As concerns the X-ray azimuthal expansion, I note that the weighted average rate, $\sim0.13\%$ yr^{-1}, is consistent with the global mean X-ray rate and that there are statistically significant azimuthal variations on angular scales of $10°$ to $90°$ (similar to those in Hughes 1997).

<div align="center">

TABLE 2
X-RAY EXPANSION RATES WITH RADIUS FOR
TYCHO'S SNR

</div>

Radial range (arcmin)	Exp Rate (% yr^{-1})	Sys Err (% yr^{-1})
$0.0 - 1.5$	0.212 ± 0.088	$(-0.090, +0.036)$
$1.5 - 2.0$	0.178 ± 0.057	$(-0.019, +0.008)$
$2.0 - 2.4$	0.124 ± 0.051	$(-0.017, +0.016)$
$2.4 - 2.8$	0.133 ± 0.033	$(-0.008, +0.006)$
$2.8 - 3.2$	0.080 ± 0.022	$(-0.000, +0.006)$
$3.2 - 3.6$	0.107 ± 0.015	$(-0.003, +0.005)$
$3.6 - 4.0$	0.117 ± 0.012	$(-0.004, +0.006)$
$4.0 - 4.4$	0.167 ± 0.012	$(-0.010, +0.008)$
$4.4 - 5.2$	0.176 ± 0.043	$(-0.004, +0.003)$

In the remainder of this section I focus on the radial variation of the X-ray expansion rate. Here the fits were carried out separately for several different annular regions about the geometric center of the remnant. Most of the radial bins were $24''$ wide although the innermost and outermost annuli were somewhat thicker. There were only two fit parameters: the fractional expansion rate and the

change in intensity. Numerical values for the expansion rate are given in Table 2 and are plotted in Figure 2 along with the change in the X-ray flux and for reference the surface brightness profile. In the bottom two panels the error bars show the statistical uncertainties, while the small boxes surrounding the data points show the range of values that come from fits using the four different expansion centers. Only for the data point closest to the remnant's center is this a significant error. Between the two epochs the X-ray flux appears to have changed only very slightly over the image of the remnant, i.e., by less than 2%. The weighted average expansion rate is $\sim0.13\%$ yr^{-1}, although I can reject the hypothesis that the expansion rate is constant with radius at more than the 99.9% confidence level ($\chi^2 = 17.65$ for 3 d.o.f.) based on the four data points near the rim (radii between 2.8 and 4.4). I find that the expansion parameter increases from $m = 0.34 \pm 0.10$ just inside the bright rim of Tycho's SNR to a value $m = 0.71 \pm 0.06$ at the outermost edge of the SNR. The rapid motion of the outermost edge is the principal cause of the non-uniform radial expansion rate. In fact, over the interior portion of the SNR, covering radii from 2.8 to 4.0, the X-ray data are consistent with an expansion parameter of $m = 0.45\pm0.04$. The large expansion rate for the outer rim, plus evidence for a slower rate further in, was also found by Hughes (1997) using an entirely different analysis technique.
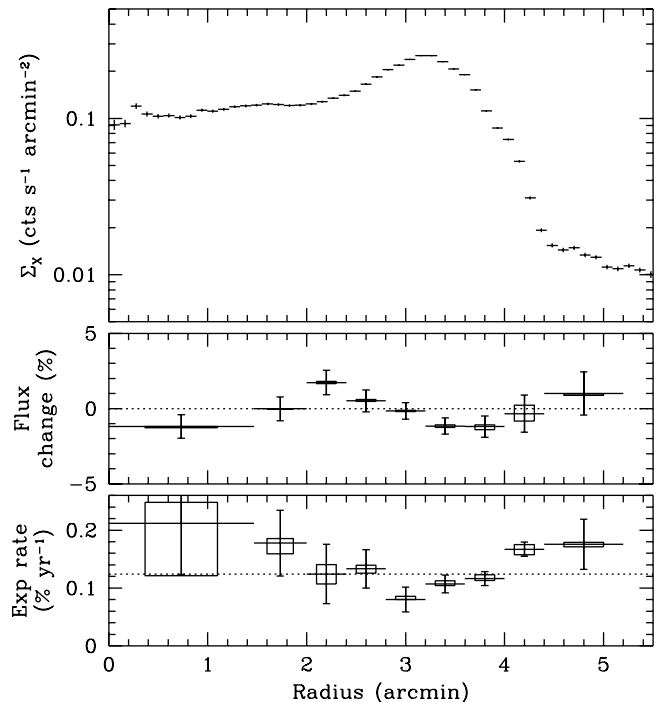

FIG. 2.— Radial X-ray surface brightness profile of Tycho's supernova remnant from the *ROSAT* HRI (top panel) and the change in X-ray flux (middle panel) and expansion rate as a function of radius (bottom panel) from a comparison of the two *ROSAT* HRI observations. The error bars show the statistical uncertainty, while the boxes that surround each data point give an estimate of the systematic uncertainty. The dashed line in the bottom panel is the global mean X-ray expansion rate.

The published radio expansion parameter of Tycho's SNR, $m = 0.471 \pm 0.028$ (R97), corresponds to the expansion of the rim. This value disagrees, by more than 3σ, with the expansion rate of the X-ray rim just derived. Tycho's SNR thus joins the two other youngest remnants

of Galactic SN (Cas A and Kepler's SNR) in showing considerably higher expansion rates in the X-ray compared to the radio (see discussion and references in H99). For Tycho's SNR it is clear that the main difference between the X-ray and radio results occurs at the remnant's outermost edge where the forward shock is plowing into the ambient interstellar medium (ISM). The slower motion of interior features (i.e., the reverse-shocked ejecta) is consistent across the radio ($m \approx 0.44$; R97) and X-ray ($m \approx 0.45$) bands.

4. DISCUSSION AND RESULTS

Numerous authors (Chevalier 1982; Dwarkadas & Chevalier 1998; Truelove & McKee 1999) have modeled the expansion rates of young supernova remnants. Dwarkadas & Chevalier (1998) in particular examined how different assumed density profiles for the SN ejecta affect the evolution of the resulting remnant, assumed to be interacting with a uniform density ISM. They considered three principal cases: a power law profile ($\rho \propto r^{-7}$), an exponential profile, and a constant density profile. The expansion parameter uniquely defines the age and radius of the remnant, conventionally expressed in scale-free variables. The constants of proportionality between the scaled values and the true physical radius and age depend on the three independent dimensional parameters: explosion energy E, ejecta mass $M_{\rm ej}$, and ambient density ρ_0. Thus, given the known size $R = 2.8(D/2.3\,{\rm kpc})\,{\rm pc}$ and age $t = 425\,{\rm yr}$ of Tycho's SNR it is possible to determine two of the three dimensional parameters. Here I assume that the ejecta mass is $1.4\,M_\odot$ and solve for the other two quantities.

The power-law profile predicts a maximum expansion parameter of $m = 0.57$ which is too low to be consistent with the X-ray expansion rate. The other two model ejecta profiles can accommodate the high rate observed for the forward shock; however, the inferred values of E and ρ_0 are quite different in the two scenarios. Compared to the uniform density case, the expansion parameter for the exponential profile model falls more rapidly with time, so that for a given value of the expansion parameter the scaled age and radius are smaller for the exponential profile. The inferred dimensional parameters for the exponential profile are $E_{51} = E/10^{51}\,{\rm erg} \approx (0.1 - 0.2)\,(M_{\rm ej}/1.4\,M_\odot)\,(D/2.3\,{\rm kpc})^2$ and $n_0 = \rho_0/\mu_{\rm H} \approx (0.004 - 0.08)\,(M_{\rm ej}/1.4\,M_\odot)\,(D/2.3\,{\rm kpc})^{-3}\,{\rm cm}^{-3}$ ($\mu_{\rm H}$ is the mean mass per hydrogen atom), rather low values for Tycho's SNR. On the other hand, more appropriate values are obtained using the uniform density ejecta model:

$E_{51} \approx (0.4 - 0.5)\,(M_{\rm ej}/1.4\,M_\odot)\,(D/2.3\,{\rm kpc})^2$ and $n_0 \approx (0.3 - 0.6)\,(M_{\rm ej}/1.4\,M_\odot)\,(D/2.3\,{\rm kpc})^{-3}\,{\rm cm}^{-3}$. These are fully consistent with the values that Hamilton, Sarazin, & Szymkowiak (1986) found in their study of Tycho's X-ray spectrum in which they also assumed a uniform density ejecta profile. Thus it appears that both the expansion of the forward shock and the X-ray emission properties of Tycho's SNR can be well explained with this simple model. What about the slower motion of the reverse-shocked ejecta?

Truelove & McKee (1999) have parameterized the evolution of both the forward and reverse shocks in young SNRs for a number of cases, including a uniform density ejecta model. For the range of scaled ages that describe the expansion of the forward shock, the reverse shock expansion parameter is $m_{\rm RS} = 0.51 - 0.63$. This rate is in reasonable agreement with the measured expansion parameter of the interior portions of Tycho's SNR ($m = 0.45 \pm 0.04$). (Although equating the motion of the ejecta to the reverse shock is not strictly correct, it serves as a reasonable first approximation.) An acceptable joint fit ($\chi^2 = 2.7$ for 1 d.o.f.) to the measured X-ray expansion parameters is obtained for best-fit values of $m \approx 0.64$ (forward) and $m \approx 0.49$ (reverse). The inferred values of E and n_0 in this case are similar to those quoted above.

The forward shock expansion rate implies a shock velocity of $4600 \pm 400\,(D/2.3\,{\rm kpc})\,{\rm km\,s}^{-1}$, which in turn implies a mean post-shock temperature of $kT_S = \frac{3}{16}\,\mu m_p v_S^2 = 25 \pm 4\,(D/2.3\,{\rm kpc})^2\,{\rm keV}$ for a mean mass per particle of $\mu = 0.61$, which assumes a fully-ionized plasma with 10% helium. This temperature is quite a bit higher than the estimate, by Hwang, Hughes, & Petre (1998), of the post-shock electron temperature of the blast wave in Tycho's SNR, $kT_e \approx 4\,{\rm keV}$. This difference most likely arises from either the non-equilibration of electron and ion temperatures at the shock front or the partition of a significant fraction of the shock energy in Tycho's SNR into relativistic particles as was recently found to be the case in SNR E0102.2−7219 (Hughes, Rakowski, & Decourchelle 2000). Discriminating between these possibilities will be the focus of a future article.

REFERENCES

Chevalier, R. A. 1982, ApJ, 258, 790
David, L. P., et al. 1998, The ROSAT High Resolution Imager (HRI) Calibration Report (http://hea-www.harvard.edu/rosat/rsdc-www/hricalrep.html)
Dwarkadas, V. V., & Chevalier, R. A. 1998, ApJ, 497, 807
Green, D. A. 1984, MNRAS, 209, 449
Hamilton, A. J. S., Sarazin, C. L., & Szymkowiak, A. E. 1986, ApJ, 300, 713
Hughes, J. P. 1997, in Proc. International Conf. on X-Ray Astronomy − ASCA 3rd Anniv.− X-Ray Imaging and Spectroscopy of Cosmic Hot Plasmas, eds. F. Makino and K. Mitsuda (Tokyo: Universal Academy), 359
Hughes, J. P. 1999, ApJ, 527, 298 (H99)
Hughes, J. P., Rakowski, C. E., & Decourchelle, A. 2000, ApJ, in press (astro-ph/0007032)

Hwang, U., Hughes, J. P., & Petre, R. 1998, ApJ, 497, 833
Kamper, K. W., & van den Bergh, S., 1978, ApJ, 224, 851
Mauche, C. W., & Gorenstein, P. 1986, ApJ, 302, 371
Predehl, P., & Schmitt, J. H. M. M. 1995, A&A, 293, 889
Reynoso, E. M., Moffett, D. A., Goss, W. M., Dubner, G. M., Dickel, J. R., Reynolds, S. P., & Giacani, E. B. 1997, ApJ, 491, 816 (R97)
Schwarz, U. J., Goss, W. M., Kalberla, P. M., & Benaglia, P. 1995, A&A, 299, 193
Smith, R. C., Kirshner, R. P., Blair, W. P., & Winkler, P. F. 1991, ApJ, 375, 652
Strom, R. G., Goss, W. M., & Shaver, P. A. 1982, MNRAS, 200, 473
Tan, S. M., & Gull, S. F. 1985, MNRAS, 216, 949
Truelove, J. K., & McKee, C. F. 1999, ApJS, 120, 299 (erratum: ApJS, 128, 403)
Vancura, O., Gorenstein, P., & Hughes, J. P. 1995, ApJ, 441, 680